NATIONAL ADVISORY COMMITTEE FOR AERONAUTICS

TECHNICAL NOTE 2336

SOME THEORETICAL CHARACTERISTICS OF TRAPEZOIDAL WINGS IN SUPERSONIC FLOW AND A COMPARISON OF SEVERAL WING-FLAP COMBINATIONS

By Robert O. Piland

Langley Aeronautical Laboratory
Langley Field, Va.

Washington
April 1951

NATIONAL ADVISORY COMMITTEE FOR AERONAUTICS

TECHNICAL NOTE 2336

SOME THEORETICAL CHARACTERISTICS OF TRAPEZOIDAL WINGS IN SUPERSONIC FLOW AND A COMPARISON OF SEVERAL WING-FLAP COMBINATIONS

By Robert O. Piland

SUMMARY

A theoretical investigation has been made by means of the linearized theory to determine some of the characteristics of a trapezoidal wing. The lift and pitching moment due to angle of attack and pitching and the lateral force and yawing moment due to rolling were derived. Charts are presented to show the variation of the derivatives, the equations for which are applicable if the inboard Mach line from a leading-edge tip intersects the trailing edge and the outboard Mach line lies ahead of the side edge. In the case of the wing with raked-in tips, the former condition is sufficient.

The trapezoidal wing may be considered a rectangular wing with a half-delta tip flap (point forward). In view of this consideration, a comparison has been made of this combination with a triangular wing with half-delta and trailing-edge flaps and with a rectangular wing with trailing-edge flaps. The triangular wing with either type of flap offered the most favorable characteristics.

INTRODUCTION

The characteristics of various wing-flap combinations suitable for supersonic flight have been the object of study in the past few years. Reference 1 has treated delta tip flaps on delta wings and found this type of flap to have some advantages. The use of tip flaps on other plan forms consequently has been considered. The present paper treats a trapezoidal plan form which may be considered a rectangular wing with a half-delta tip flap. Characteristics of this wing in roll and yaw have been treated in references 2 and 3, respectively.

The lift and pitching moment due to angle of attack and pitching and the lateral force and yawing moment due to rolling are derived for the trapezoidal wing with raked-out tips. These characteristics for the

reverse wing (raked-in tips) are discussed on the basis of relations derived in reference 4 concerning a wing and its reverse.

The derivatives are applicable when the inboard Mach line from a leading-edge tip crosses the trailing edge and the outboard Mach line lies ahead of the side edge. In the case of the reverse wing, a sufficient condition is that the inboard Mach line from a leading-edge tip intersects the trailing edge.

Theoretical material of references 1, 2, 5, 6, 7, and 8 has been used to compare the effectiveness of various wing-flap combinations. The lift due to flap deflection and the rolling effectiveness of half-delta tip (point forward) and trailing-edge flaps on rectangular and triangular wings are compared.

Since the completion of this investigation, it has been brought to the attention of the author that expressions for the lift and pitching moment due to angle of attack for the trapezoidal wing have been derived previously in reference 9 and that also in reference 10 the expression for the lift has been derived.

SYMBOLS

x,y,z	rectangular coordinates (see fig. 2)
u,v,w	incremental flight velocities along x-, y-, and z-axes, respectively
V	undisturbed flight velocity
p,q	angular velocities about x- and y-axes, respectively (see fig. 2)
a	speed of sound
M	free-stream Mach number (V/a)
$\beta = \sqrt{M^2 - 1}$	
μ	Mach angle $\left(\sin^{-1} \frac{1}{M}\right)$
α	wing angle of attack in steady flight $(-w/V)$
α'	local inclination of airfoil surface with respect to free stream
δ	angle of flap deflection

c_r wing root chord

$\bar{c}$ wing mean aerodynamic chord

c_f chord of flap

b span of wing

b_f span of two flaps

Λ sweep angle of flap

$m = \cot \Lambda$

$h = \frac{b}{2} - mc_r$

S total wing area

S_f area of two flaps

S_w region of integration over part of wing surface (see fig. 3)

A aspect ratio $\left(\frac{b^2}{S} = \frac{b^2}{c_r(b - mc_r)}\right)$

$n = \frac{c_r}{\beta b}$

ρ mass density of air

φ disturbance velocity potential on upper surface of airfoil

ξ, η auxiliary variables which replace x and y, respectively, (see fig. 3)

Δp pressure difference between upper and lower surfaces of airfoil, positive in direction of lift

$P = \frac{\Delta p}{\frac{1}{2}\rho V^2}$

F suction force per unit length of edge

L force parallel to z-axis (see fig. 2)

C_L lift coefficient $\left(\frac{L}{\frac{1}{2}\rho V^2 S}\right)$

Y force parallel to y-axis (see fig. 2)

C_Y lateral-force coefficient $\left(\frac{Y}{\frac{1}{2}\rho V^2 S}\right)$

L', M, N moments about x-, y-, and z-axes, respectively (see fig. 2)

C_l rolling-moment coefficient $\left(\frac{L'}{\frac{1}{2}\rho V^2 Sb}\right)$

C_m pitching-moment coefficient about center of root chord $\left(\frac{M}{\frac{1}{2}\rho V^2 S\bar{c}}\right)$

C_n yawing-moment coefficient $\left(\frac{N}{\frac{1}{2}\rho V^2 Sb}\right)$

$$E''(\beta m) = \frac{1}{E'(\beta m)}$$

$E'(\beta m)$ complete elliptic integral of the second kind with modulus $k = \sqrt{1 - \beta^2 m^2}$; $\left(\int_0^{\pi/2} \sqrt{1 - k^2 \sin^2 z}\, dz\right)$

$$I(\beta m) = \frac{2(1 - \beta^2 m^2)}{\left(2 - \beta^2 m^2\right) E'(\beta m) - \beta^2 m^2 F'(\beta m)}$$

$F'(\beta m)$ complete elliptic integral of the first kind with modulus k; $\left(\int_0^{\pi/2} \frac{dz}{\sqrt{1 - k^2 \sin^2 z}}\right)$

Subscripts:

R, L right and left edge of wing, respectively

Whenever α, q, p, δ are used as subscripts a nondimensional derivative is indicated and this derivative is the slope through zero.

For example:

$$C_{L_\alpha} = \left(\frac{\partial C_L}{\partial \alpha}\right)_{\alpha \to 0} \qquad C_{m_q} = \left(\frac{\partial C_m}{\partial \frac{q\bar{c}}{2V}}\right)_{\frac{q\bar{c}}{2V} \to 0}$$

$$C_{l_p} = \left(\frac{\partial C_l}{\partial \frac{pb}{2V}}\right)_{\frac{pb}{2V} \to 0} \qquad C_{L_\delta} = \left(\frac{\partial C_L}{\partial \delta}\right)_{\delta \to 0}$$

ANALYSIS

Scope

The trapezoidal wing for which the equations are derived is shown in figure 1. The application of these equations to the reverse wing (raked-in tips) by means of relations derived in reference 4 is discussed. The equations are applicable when the inboard Mach line from a leading-edge tip intersects the trailing edge and the outboard Mach line lies ahead of the side edge. In the case of the reverse wing it is only necessary that the inboard Mach line from a tip intersect the trailing edge.

All results are subject to the inherent restrictions and limitations of the linearized thin-airfoil theory for supersonic flow. Equations are derived with respect to a body system of coordinate axes, as indicated in figure 2.

Method

The stability derivatives were obtained by integrating forces and moments over the wing. In the case of vertical and pitching motion, the forces and moments were due entirely to pressures acting normal to the wing surface. In the case of rolling, lateral forces and moments will be produced by unbalanced suction forces along the side edges. The problem, therefore, is the determination of the pressures on the wing surface and the suction forces along the tip edges.

By means of Bernoulli's equation, the pressures are obtained as a function of the velocity potential; therefore, by using Evvard's method (reference 11) to determine the potential, the pressures may be obtained.

The potentials are also used in the determination of the tip suction forces by a method from reference 7.

Evvard's method is an extension of Puckett's (reference 12) to include the effect of a tip with a subsonic edge. For a point in the tip region affected by an external independent field, the potential function may be obtained by integrating the elementary-source solution over an appropriate area as illustrated in figure 3. As applied to this wing, the method is applicable if the Mach line from the tip leading edge intersects the trailing edge of the wing so as to preserve the concept of independent external fields. Therefore, from equation (15) of reference 11

$$\varphi(x,y) = \frac{V}{\pi}\int_{S_w}\int \frac{\alpha'\, d\xi\, d\eta}{\sqrt{(x-\xi)^2 - \beta^2(y-\eta)^2}} \tag{1}$$

where α' represents the local angle of attack of the airfoil surface at point ξ,η. The limits of the integral are indicated in figure 3. For the region inboard of the tip, Puckett's method is applicable. The potentials for the various motions in this region were obtained from reference 6. After φ is obtained, the derivative is taken in the flight direction, and this derivative is substituted in Bernoulli's equation, the following expression for the pressure difference on the wing surface is obtained:

$$\Delta p = 2\rho V \frac{\partial \varphi}{\partial x} \tag{2}$$

Derivation of the Derivatives

Derivatives C_{L_α} and C_{L_q}.- The potential φ in the tip region (see fig. 3) for steady vertical and pitching motion about a lateral axis through the midchord may be determined from equation (1). Substitute for α the local slope of the airfoil surface with respect to the free-stream direction, that is,

$$\alpha' = \alpha + \frac{\xi - \frac{c_r}{2}}{V} q \tag{3}$$

where α is the angle of attack in the absence of pitching. When the indicated double integration is performed, the potential is obtained. The pressure coefficient is then realized by use of equation (2). The potential and pressure coefficient inboard of the tip are given in

reference 6. Integrating these pressures over the respective regions (see fig. 4) and converting to nondimensional form gives the lift coefficient. The derivatives C_{L_α} and C_{L_q} are then obtained by differentiation of the coefficient with respect to α and $q\bar{c}/2V$, respectively.

Derivatives C_{m_α} and C_{m_q}.- The derivatives C_{m_α} and C_{m_q} involve the use of the pressure coefficients obtained for angle of attack and pitching. The pitching moment about the middle of the root chord is obtained by integrating the product of pressures and moment arms over the surface of the wing.

$$C_m = \frac{1}{\frac{1}{2}\rho V^2 S\bar{c}} \iint_S P\left(\frac{c_r}{2} - x\right) dx\, dy \tag{4}$$

The derivatives C_{m_α} and C_{m_q} are then obtained by differentiating with respect to α and $q\bar{c}/2V$, respectively.

Derivatives C_{Y_p} and C_{n_p}.- The lateral force and yawing moment relative to body axes in a rolling motion for a thin wing without dihedral arise entirely from suction forces on the wing side edges. The present case is treated in the same manner as the triangular wing in reference 7 which is based on the method of reference 13. The induced velocity components due to rolling u_1 and angle of attack u_2 are as follows:

$$u_1 = \left(\frac{\partial \varphi}{\partial x}\right)_p = \frac{p}{\pi\beta}\left\{(h + y)\cos^{-1}\left[\frac{1 - \beta m}{1 + \beta m} + \frac{2\beta y}{x(1 + \beta m)}\right]\right\} +$$

$$\frac{2\left[3\beta^2 mh(\beta m + 1) + 3\beta y(\beta^2 m^2 + 1) + 2\beta m(\beta y - 2x)\right]}{3\beta(\beta m + 1)^2}\sqrt{\frac{x + \beta y}{\beta m x - \beta y}} \tag{5}$$

$$u_2 = \left(\frac{\partial \varphi}{\partial x}\right)_w = \frac{\alpha V}{\pi\beta}\left\{\cos^{-1}\left[\frac{1 - \beta m}{1 + \beta m} + \frac{2\beta y}{x(1 + \beta m)}\right] + \frac{2\beta m}{1 + \beta m}\sqrt{\frac{x + \beta y}{\beta m x - \beta y}}\right\} \tag{6}$$

where the subscripts p and w indicate the contributions caused by rolling and vertical motion, respectively.

By following the procedure of reference 7, the suction force per unit length of edge is found to be

$$F = x\,\frac{4\rho\sqrt{1-\beta^2m^2}}{\pi\beta(\beta m+1)}\left\{(\alpha V)^2 \pm 2\alpha V p\left[\frac{x}{3\beta}(3\beta m-1)+h\right] + p^2\left[\frac{x}{3\beta}(3\beta m-1)+h\right]^2\right\} \tag{7}$$

where the + and - signs refer to the suction forces on the right and left side edges, respectively. The lateral component of this suction force is given by

$$Y = \int_0^{c_r} \left(F_R - F_L\right)dx \tag{8}$$

By converting to nondimensional form and by taking the derivative of C_Y with respect to $pb/2V$, C_{Y_p} is obtained.

The yawing moment of the leading-edge suction about the midchord point is

$$N = -\int_0^{c_r\sqrt{m^2+1}} \left(F_R - F_L\right)\left(\frac{hm-\frac{c_r}{2}}{\sqrt{m^2+1}} + x\sqrt{m^2+1}\right) d\left(x\sqrt{m^2+1}\right) \tag{9}$$

Again by converting to nondimensional form and by taking the derivative with respect to $pb/2V$, C_{n_p} is obtained.

RESULTS AND DISCUSSION

General.- The velocity potentials and pressure coefficients for the trapezoidal wing for the motions considered are given in table I. The derivatives obtained are presented in table II. Figure 5 indicates the range of applicability of the equations. The curve was obtained from the relation

$$\beta A \leqq \left(\frac{2\beta m}{1-\sqrt{1-\frac{4\beta m}{\beta A}}}\right)^2 \tag{10}$$

which physically means that the inboard Mach line from the tip leading edge must intersect the wing trailing edge. The condition that the outboard Mach line from the leading-edge tip lies ahead of the leading edge ($\beta m < 1$) must also be satisfied.

Lift.- The variation of βC_{L_q} and βC_{L_α} with βm for various values of βA is shown in figure 6.

Pitching moment.- The variation of the derivatives βC_{m_α} and $-\beta C_{m_q}$ with βm for different values of βA is shown in figure 7. The wing is considered to be pitching about the midpoint of the root chord; the pitching moments are taken about this point. Figure 7 shows that βC_{m_α} becomes zero at $\beta m = \frac{1}{3}$, regardless of the value of βA. This condition is also obvious from the equation in table II. For values of βm greater than $1/3$, βC_{m_α} becomes increasingly negative and, therefore, greater stability is indicated. This increase in stability is caused by the movement of the center of pressure behind the middle of the root chord. The derivative βC_{m_α} is positive for all rectangular cases ($\beta m = 0$). A marked effect of varying the aspect ratio or sweep of the side edge on βC_{m_q} is seen; whereas, in comparison, βC_{m_q} for the rectangular wing is a constant for all values of βA.

Lateral force and yawing moment.- The variation of the derivative C_{Y_p}/α with βm for various values of βA is shown in figure 8. The derivative for all values of βA becomes zero at $\beta m = 1$. This condition can be attributed to the fact that the nature of the flow at $\beta m < 1$ is inherently subsonic and becomes supersonic when the Mach line crosses the side edge of the wing, that is at $\beta m = 1$.

The derivatives discussed so far have all been functions of the parameters βm and βA. The derivative C_{n_p}/α, however, is a function of m^2 as well as βm and βA; therefore, the variation of this derivative with Mach number is shown for a group of specific wings in figure 9. The Mach number at which C_{n_p}/α for the various wings becomes zero corresponds to a value of 1 for βm. The reason for this value of zero for the derivative is the same as that noted for C_{Y_p}.

Reverse trapezoidal wings (raked-in tips).- The characteristics of the trapezoidal wing with raked-in tips may be obtained from the equations for the raked-out-tip wing by utilizing the relations obtained in reference 4. The relations for this plan form are based on the assumption that the Kutta-Joukowski condition is imposed. With respect to a system of body axes, the relations between the characteristics of a trapezoidal wing and its reverse (primed derivatives) may be written

$$\left.\begin{aligned} C_{L_\alpha} &= C_{L_\alpha}' \\ C_{m_\alpha} &= \frac{C_{L_q}'}{2} \\ C_{L_q} &= 2C_{m_\alpha}' \\ C_{m_q} &= C_{m_q}' \end{aligned}\right\} \tag{11}$$

The derivatives C_{Y_p} and C_{n_p} for the reverse wing become zero, since there is no subsonic leading edge and, therefore, no leading-edge suction force.

Comparative effectiveness of half-delta and trailing-edge flaps.- A comparison of the effectiveness of half-delta tip (point forward) and trailing-edge flaps on rectangular and triangular plan forms is made on the basis of equal values of their respective lift-curve slopes. The trapezoidal wing may be considered a rectangular wing with a half-delta tip flap (point forward). The plan forms considered are a triangular and trapezoidal wing with half-delta tip flaps and a triangular and rectangular wing with trailing-edge outboard flaps. The comparison is valid for a range of Mach numbers for which βm is less than 1.

Comparisons of the lift due to flap deflection C_{L_δ} and of the rolling effectiveness $\frac{pb}{2V}\Big/\delta$ are made for the various combinations. The rolling effectiveness is given by the ratio C_{l_δ}/C_{l_p}. The expressions for C_{L_δ}, C_{l_δ}, C_{l_p}, and C_{L_α} for the plan forms are presented in table III with their range of applicability and the source from which they were obtained.

Figures 10 and 11 present the variation of βC_{L_δ} with βC_{L_α} and $\frac{pb}{2V}\Big/\delta$ with βC_{L_α}, respectively; the condition is specified that $\frac{S_f}{S} = 0.1$. Two curves for different combinations of c_f/c_r and b_f/b are shown for the rectangular wing. Both, however, satisfy the condition that $\frac{S_f}{S} = 0.1$. The case presented for the triangular wing with trailing-edge flaps is for a value of $\frac{b_f}{b}_{S_f} = 0.4$ and a value of $\frac{c_f}{c_r} = 0.155$ which meets the condition that $\frac{S_f}{S} = 0.1$. Other combinations for both the rectangular and triangular wings with trailing-edge flaps could be chosen that would meet the conditions specified but they would not alter the qualitative conclusions drawn.

The two curves of βC_{L_δ} for the rectangular case (fig. 10) illustrate the obvious effect of flap aspect ratio on lift, that is, the higher the aspect ratio the higher the lift. The half-delta tip flap on the triangular wing gives considerably higher values of βC_{L_δ} than a like control on the trapezoidal wing. Since the expression for βC_{L_δ} is not affected by plan form, the explanation lies in the fact that, to obtain a given βC_{L_α}, a higher value of βm is required for the triangular wing than for the trapezoidal wing.

Figure 11 presents the rolling effectiveness of the various plan forms. The half-delta tip flap exhibits the ability to maintain its rolling effectiveness through the range of βC_{L_α} considered. This condition can probably be attributed to the inherently low flap aspect ratio of the half-delta flaps. This fact is substantiated by the variation of the rolling effectiveness of the two rectangular cases with flap aspect ratio which shows a tendency for the rectangular wings to maintain their effectiveness better as the flap aspect ratio is decreased.

The trapezoidal wing with half-delta tip flap not only maintains its rolling effectiveness generally but actually increases its effectiveness at the higher values of βC_{L_α}. The physical reason for this condition is not readily apparent and its practical use, if any, remains to be seen.

By using figures 10 and 11, an idea of the relative effects of βC_{l_δ} and βC_{l_p} on the rolling effectiveness of the various combinations may be obtained. Figure 11 shows that the rolling effectiveness of the rectangular wing with trailing-edge flaps drops off much more rapidly as βC_{L_α} is increased than the triangular wing with trailing-edge flaps. Since figure 10 indicates that for these wing-flap combinations the values of βC_{L_δ} are comparable, a much more rapid increase in βC_{l_p} for the rectangular case is evident. Contrastingly, the values of βC_{L_δ} of the rectangular and trapezoidal combinations differ greatly over a large part of the range but approach the same value as βC_{L_α} approaches 4. In figure 11 similar trends are noted for the rectangular and trapezoidal wing and indicate that the values of βC_{l_p} are of the same order for the two wings.

A comparison of the triangular and trapezoidal combinations with half-delta flaps shows that the rolling effectiveness of the triangular case is higher by an almost constant amount throughout the range. This almost constant difference is the result of the facts that, as βC_{L_α} increases, the βC_{L_δ} curves converge, although for the lower values

of βC_{L_α} $\left(\beta C_{L_\alpha} \lessapprox 3\right)$ considerably lower values of BC_{L_δ} are evident for the trapezoidal case, and, since the rolling-effectiveness curves remain fairly level, the curves of βC_{l_p} are obviously diverging with the triangular case increasing slower than the trapezoidal case.

CONCLUDING REMARKS

The trapezoidal wing with raked-out tips was investigated theoretically to determine some of its characteristics. The lift and pitching moment due to angle of attack and pitching and the lateral force and yawing moment due to rolling were derived. The reverse wing (raked-in tips) was discussed and previously derived expressions relating the characteristics of a wing and its reverse are given. The lateral force and yawing moment due to rolling are zero for the reverse wing. The equations are applicable when the inboard Mach line from a leading-edge tip intersects the trailing edge and the outboard Mach line lies ahead of the side edge. In the case of the wing with raked-in tips the former condition is sufficient.

A comparison of the lift due to flap deflection and the rolling effectiveness for half-delta tip (point forward) and trailing-edge flaps on various plan forms was made. The following conclusions were reached:

1. In general the triangular wing with either half-delta tip or trailing-edge flaps offered the most favorable characteristics.

2. The half-delta tip flaps (point forward) showed the ability to maintain their rolling effectiveness throughout the range considered.

3. The half-delta tip flaps (point forward) on trapezoidal wings had a tendency to increase its rolling effectiveness at the higher values of βC_{L_α} considered. (βC_{L_α} is defined as the product of the Mach number parameter and the lift-curve slope.)

Langley Aeronautical Laboratory
National Advisory Committee for Aeronautics
Langley Field, Va., January 30, 1951

REFERENCES

1. Tucker, Warren A., and Nelson, Robert L.: Theoretical Characteristics in Supersonic Flow of Two Types of Control Surfaces on Triangular Wings. NACA Rep. 939, 1949.

2. Jones, Arthur L., and Alksne, Alberta: The Damping Due to Roll of Triangular, Trapezoidal, and Related Plan Forms in Supersonic Flow. NACA TN 1548, 1948.

3. Jones, Arthur L., and Alksne, Alberta: The Yawing Moment Due to Sideslip of Triangular, Trapezoidal, and Related Plan Forms in Supersonic Flow. NACA TN 1850, 1949.

4. Harmon, Sidney M.: Theoretical Relations between the Stability Derivatives of a Wing in Direct and in Reverse Supersonic Flow. NACA TN 1943, 1949.

5. Lagerstrom, P. A., and Graham, Martha E.: Linearized Theory of Supersonic Control Surfaces. Jour. Aero. Sci., vol. 16, no. 1, Jan. 1949, pp. 31-34.

6. Harmon, Sidney M.: Stability Derivatives at Supersonic Speeds of Thin Rectangular Wings with Diagonals ahead of Tip Mach Lines. NACA Rep. 925, 1949.

7. Ribner, Herbert S., and Malvestuto, Frank S., Jr.: Stability Derivatives of Triangular Wings at Supersonic Speeds. NACA Rep. 908, 1948.

8. Tucker, Warren A., and Nelson, Robert L.: Theoretical Characteristics in Supersonic Flow of Constant-Chord Partial-Span Control Surfaces on Rectangular Wings Having Finite Thickness. NACA TN 1708, 1948.

9. Jones, Arthur L., Sorenson, Robert M., and Lindler, Elizabeth E.: The Effects of Sideslip, Aspect Ratio, and Mach Number on the Lift and Pitching Moment of Triangular, Trapezoidal, and Related Plan Forms in Supersonic Flow. NACA TN 1916, 1949.

10. Heaslet, Max. A., Lomax, Harvard, and Jones, Arthur L.: Volterra's Solution of the Wave Equation as Applied to Three-Dimensional Supersonic Airfoil Problems. NACA Rep. 889, 1947.

11. Evvard, John C.: Distribution of Wave Drag and Lift in the Vicinity of Wing Tips at Supersonic Speeds. NACA TN 1382, 1947.

12. Puckett, Allen E.: Supersonic Wave Drag of Thin Airfoils. Jour. Aero. Sci., vol. 13, no. 9, Sept. 1946, pp. 475-484.

13. Brown, Clinton E.: Theoretical Lift and Drag of Thin Triangular Wings at Supersonic Speeds. NACA Rep. 839, 1946.

TABLE I

THE VELOCITY POTENTIALS AND PRESSURE COEFFICIENTS FOR THE MOTIONS AND REGIONS INDICATED

Motion	Potential or coefficient		
Vertical	φ	$\frac{V\alpha x}{\beta}$	$\frac{\alpha V}{\pi\beta}\left\{x\cos^{-1}\left[\frac{1-\beta m}{1+\beta m}+\frac{2\beta y}{x(1+\beta m)}\right]+\frac{2\sqrt{(\beta mx-\beta y)(x+\beta y)}}{1+\beta m}\right\}$
	P	$\frac{4\alpha}{\beta}$	$\frac{4\alpha}{\pi\beta}\left\{\cos^{-1}\left[\frac{1-\beta m}{1+\beta m}+\frac{2\beta y}{x(1+\beta m)}\right]+\frac{2\beta m}{1+\beta m}\sqrt{\frac{x+\beta y}{\beta mx-\beta y}}\right\}$
Pitching	φ	$\frac{qx(x-c_r)}{2\beta}$	$\frac{q}{3\pi\beta}\left\{\frac{3x}{2}(x-c_r)\cos^{-1}\left[\frac{1-\beta m}{1+\beta m}+\frac{2\beta y}{x(1+\beta m)}\right]+\frac{2\beta y+x(3\beta m+5)-3c_r(\beta m+1)}{(\beta m+1)^2}\sqrt{(x+\beta y)(\beta mx-\beta y)}\right\}$
	P	$\frac{4q\left(x-\frac{c_r}{2}\right)}{\beta V}$	$\frac{4q}{3\pi\beta V}\left\{3\left(x-\frac{c_r}{2}\right)\cos^{-1}\left[\frac{1-\beta m}{1+\beta m}+\frac{2\beta y}{x(1+\beta m)}\right]+\frac{-2\beta y(\beta m+3)+2\beta mx(3\beta m+5)-3\beta mc_r(\beta m+1)}{(\beta m+1)^2}\sqrt{\frac{x+\beta y}{\beta mx-\beta y}}\right\}$
Rolling	φ	$\frac{pyx}{\beta}$	$\frac{p}{\pi}\left\{\frac{x}{\beta}(h+y)\cos^{-1}\left[\frac{1-\beta m}{1+\beta m}+\frac{2\beta y}{x(1+\beta m)}\right]+\frac{2}{\beta(1+\beta m)}\left[h+\frac{y(3\beta m+1)}{3(\beta m+1)}-\frac{2x}{3\beta(\beta m+1)}\right]\sqrt{(x+\beta y)(\beta mx-\beta y)}\right\}$
	P	$\frac{4py}{\beta V}$	$\frac{4p}{\pi\beta V}\left\{(h+y)\cos^{-1}\left[\frac{1-\beta m}{1+\beta m}+\frac{2\beta y}{x(1+\beta m)}\right]+\frac{2\left[3\beta^2mh(\beta m+1)+3\beta y(\beta^2m^2+1)+2\beta m(\beta y-2x)\right]}{3\beta(\beta m+1)^2}\sqrt{\frac{x+\beta y}{\beta mx-\beta y}}\right\}$

TABLE II

STABILITY DERIVATIVES OF THE TRAPEZOIDAL WING WITH RAKED-OUT TIPS

Derivative	Formula
	Vertical motion
βC_{L_α}	$2\beta An\left[2 - n(\beta m + 1)\right]$
βC_{L_q}	$\frac{2n(\beta m + 1)}{3\left(1 - \frac{4}{3}\beta mn\right)}$
	Pitching motion
βC_{m_α}	$\frac{n(1 - 3\beta m)}{3\left(1 - \frac{4}{3}\beta mn\right)}$
βC_{m_q}	$\frac{-2(1 - \beta mn)^2}{3\left(1 - \frac{4}{3}\beta mn\right)^2}$
	Rolling motion
$\frac{C_{Y_p}}{\alpha}$	$\frac{64\beta An^2}{\pi}\frac{\sqrt{1 - \beta^2 m^2}}{1 + \beta m}\left[\frac{1}{4} - \frac{n}{3}\left(\frac{\beta m}{2} + \frac{1}{3}\right)\right]$
$\frac{-C_{n_p}}{\alpha\beta}$	$\frac{32\beta An^2}{\pi}\sqrt{\frac{1 - \beta m}{1 + \beta m}}\left\{\frac{m^2}{4\beta m} + \frac{n}{3}\left[\frac{-m^2(3\beta m + 1)}{3\beta m} + \frac{1}{4}\right] + \frac{n^2}{18}\left[m^2(3\beta m + 1) - 1\right]\right\}$

NACA

TABLE III

DERIVATIVES FOR THE VARIOUS WING-FLAP COMBINATIONS

Derivative	Source	Formula
Triangular wing with half-delta flap $\left(\beta m \leqq 1;\ \frac{c_f}{c_r} \leqq \frac{1}{2}\right)$		
βC_{L_δ}	Reference 5	$4\sqrt{\beta m}$
βC_{L_α}	Reference 7	$\frac{\pi \beta A}{2} E''(\beta m)$
βC_{l_δ}	Reference 5	$2\sqrt{\beta m}\,\frac{S_f}{S}\left[1 - \frac{c_f}{3\beta b}(3\beta m + 1)\right]$
βC_{l_p}	Reference 7	$\frac{-\pi \beta A}{32} I(\beta m)$
Triangular wing with trailing-edge flap $\left(\beta m \leqq 1;\ \frac{1}{\beta m}\frac{c_f}{c_r} \leqq \frac{b_f}{b} \leqq 1\right)$		
βC_{L_δ}	Reference 1	$4\left[2\,\frac{b_f}{b}\,\frac{c_f}{c_r} - \frac{1 + \beta m}{2\beta m}\left(\frac{c_f}{c_r}\right)^2\right]$
βC_{l_p}	Reference 1	$2\left[\left(2 - \frac{b_f}{b}\right)\frac{b_f}{b}\,\frac{c_f}{c_r} - \frac{1 + \beta m}{2\beta m}\left(\frac{c_f}{c_r}\right)^2 + \frac{3\beta^2 m^2 + 6\beta m - 1}{24\beta^2 m^2}\left(\frac{c_f}{c_r}\right)^3\right]$
Rectangular wing with half-delta flap $\left(\beta m < 1;\ \beta A \leqq \left(\frac{2\beta m}{1 - \sqrt{1 - \frac{4\beta m}{\beta A}}}\right)^2\right)$		
βC_{L_δ}	Reference 5	$4\sqrt{\beta m}$
βC_{L_α}	Present paper	$2\beta A n\left[2 - n(\beta m + 1)\right]$
βC_{l_δ}	Reference 5	$2\sqrt{\beta m}\,\frac{S_f}{S}\left[1 - \frac{n}{3}(3\beta m + 1)\right]$
βC_{l_p}	Reference 2	$-\beta A n\left[\frac{2}{3} - n(\beta m + 1) + \frac{n^2}{3}(\beta m + 1)(3\beta m + 1) + \frac{n^3}{12}(\beta m + 1)^2(1 - 5\beta m)\right]$
Rectangular wing with trailing-edge flap $\left(\beta A \geqq 1;\ \frac{2}{\beta A}\left(\frac{c_f}{c_r}\right) \leqq \frac{b_f}{b} \leqq 1\right)$		
βC_{L_δ}	Reference 8	$\frac{4S_f}{S} - \frac{2}{\beta A}\left(\frac{c_f}{c_r}\right)^2$
βC_{L_α}	Reference 6	$4 - \frac{2}{\beta A}$
βC_{l_δ}	Reference 8	$\frac{S_f}{S}\left(2 - \frac{b_f}{b}\right) - \frac{1}{\beta A}\left(\frac{c_f}{c_r}\right)^2 - \frac{1}{6\beta^2 A^2}\left(\frac{c_f}{c_r}\right)^3$
βC_{l_p}	Reference 6	$-\left(\frac{2}{3} - \frac{1}{\beta A} + \frac{1}{3\beta^2 A^2} + \frac{1}{12\beta^3 A^3}\right)$

NACA

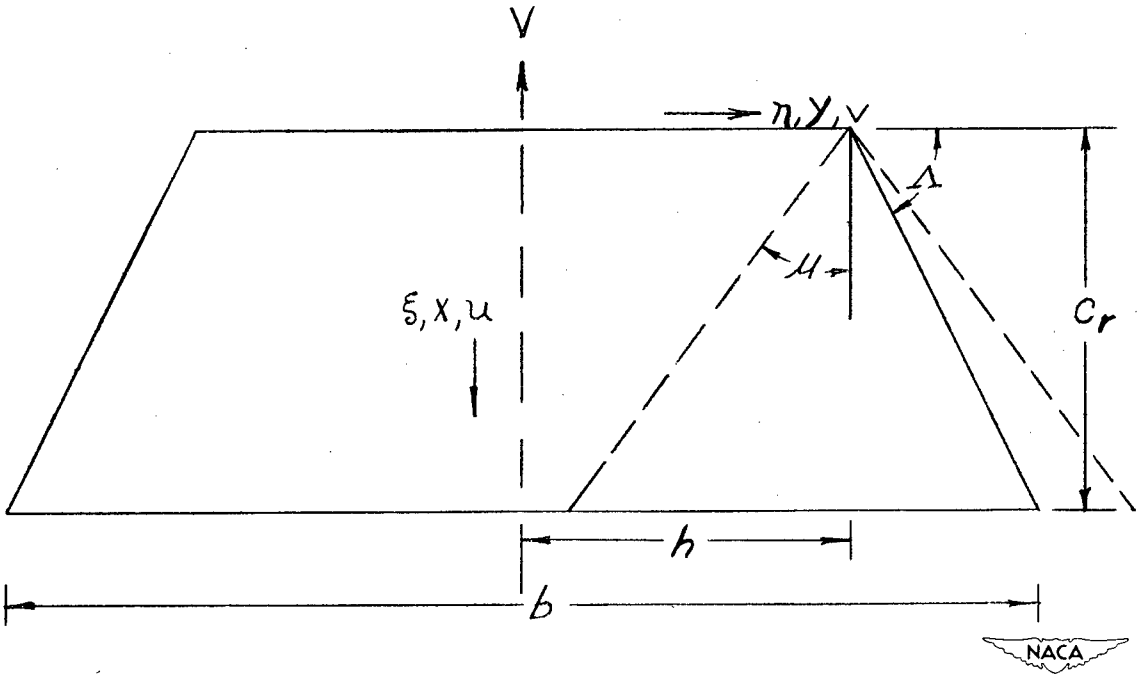

Figure 1.- Axes and notation used in analysis.

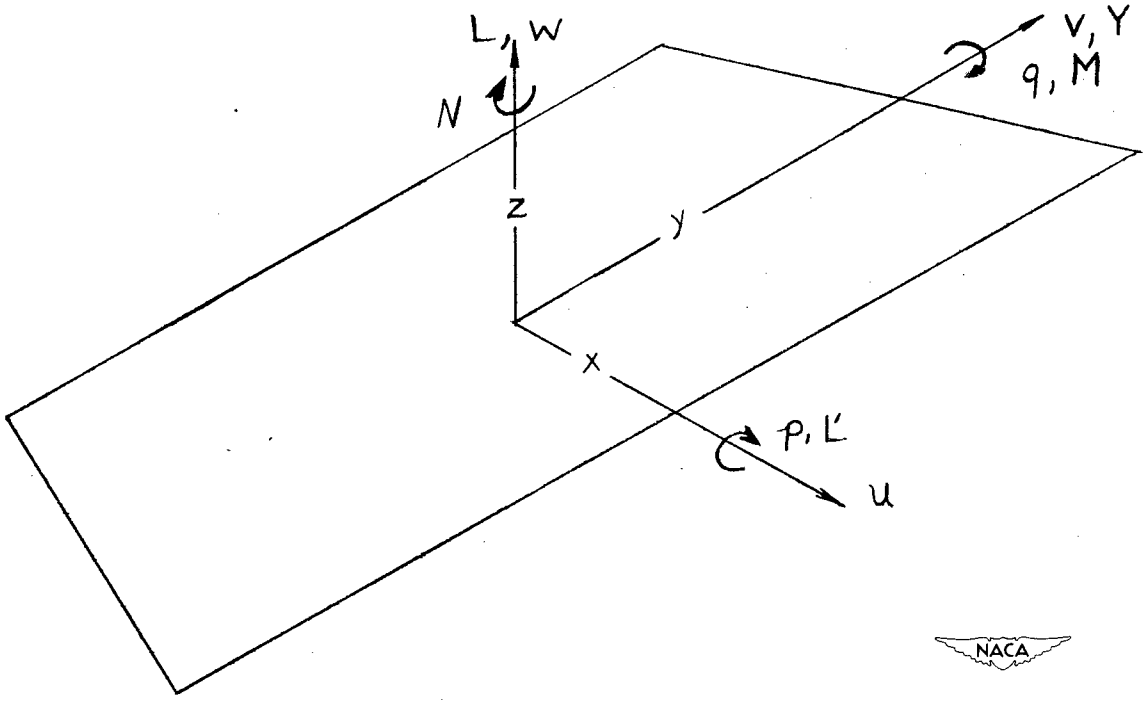

Figure 2.- Body axes with origin at center of root chord.

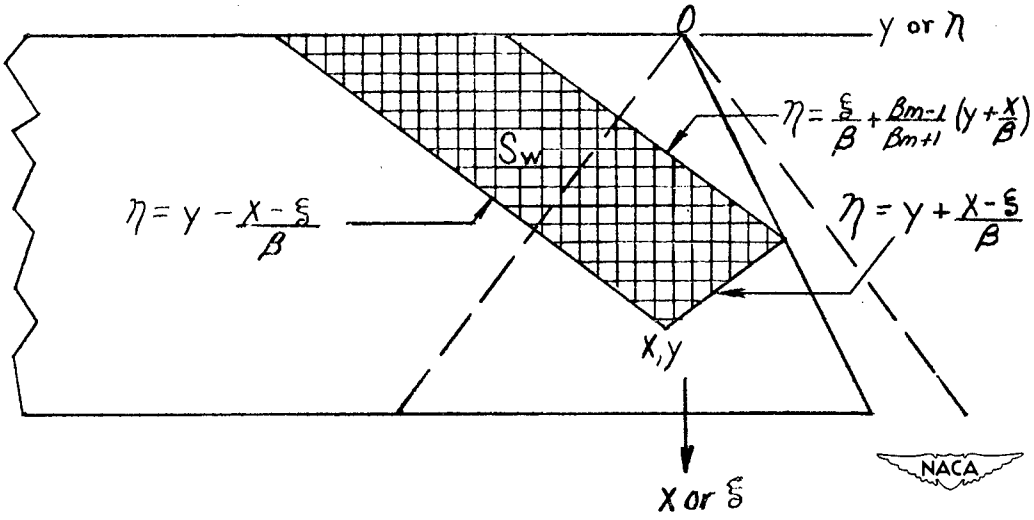

Figure 3.- Region of integration for obtaining velocity potential function in tip region.

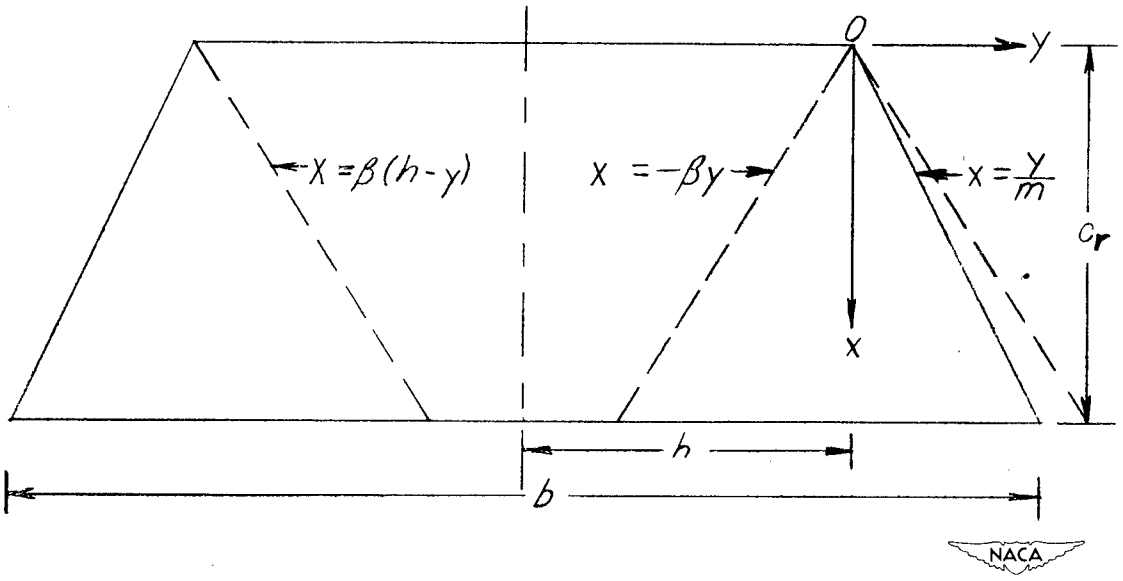

Figure 4.- Limits used in integrating pressures over the wing.

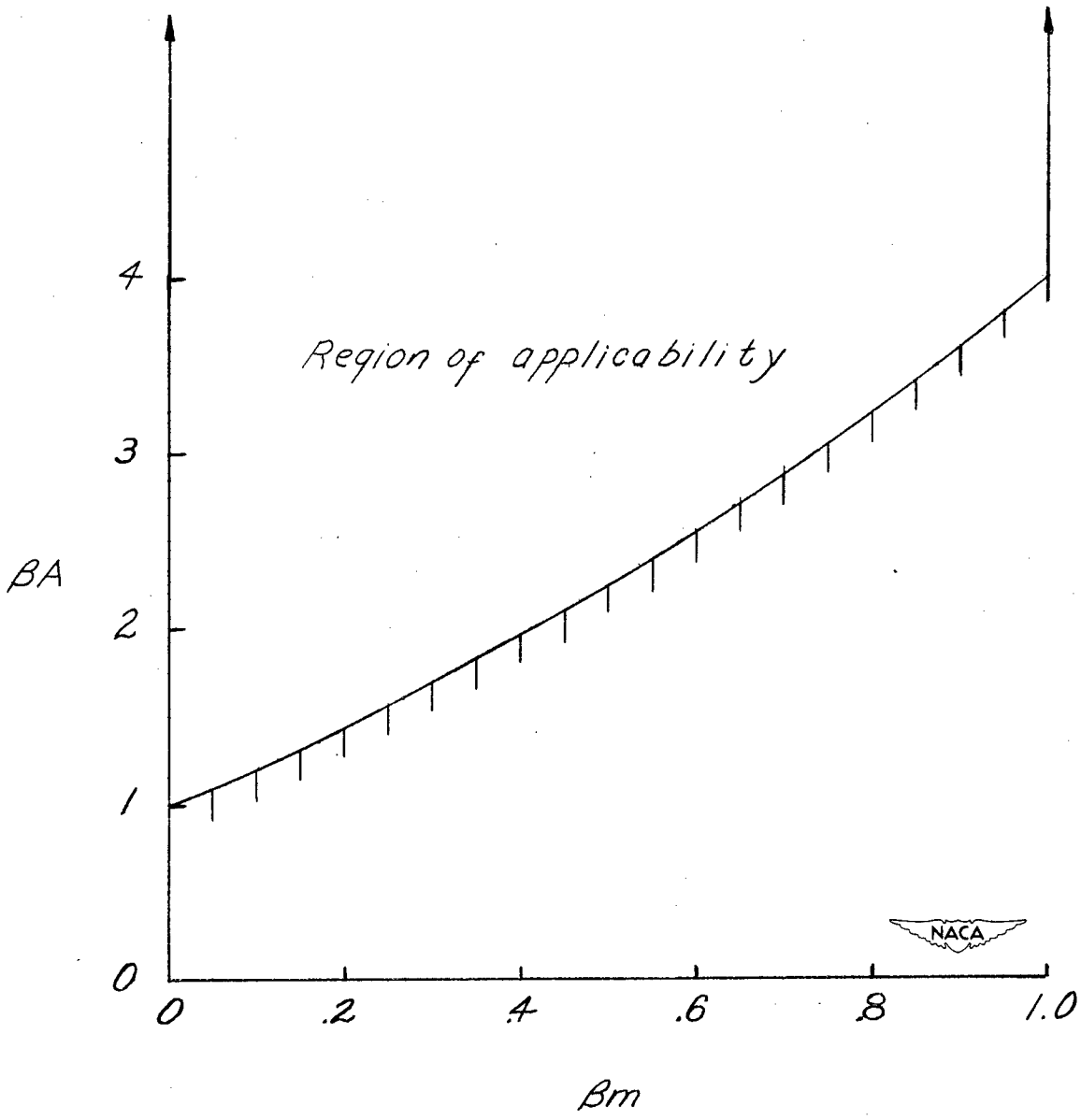

Figure 5.- Range of applicability of the derivatives for the trapezoidal wing.

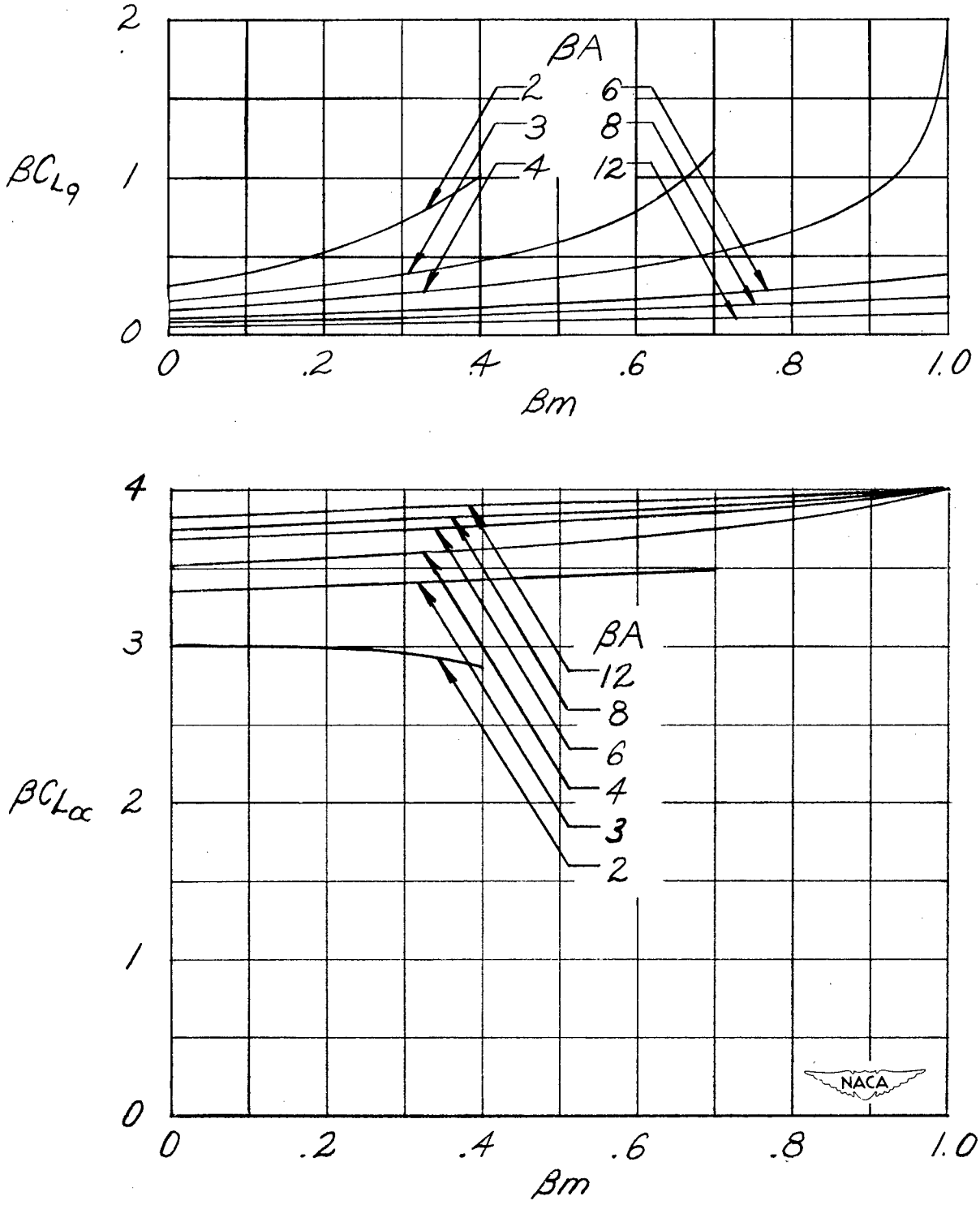

Figure 6.- Variation of βC_{L_α} and βC_{L_q} with βm for various values of of βA for trapezoidal wing with raked-out tips.

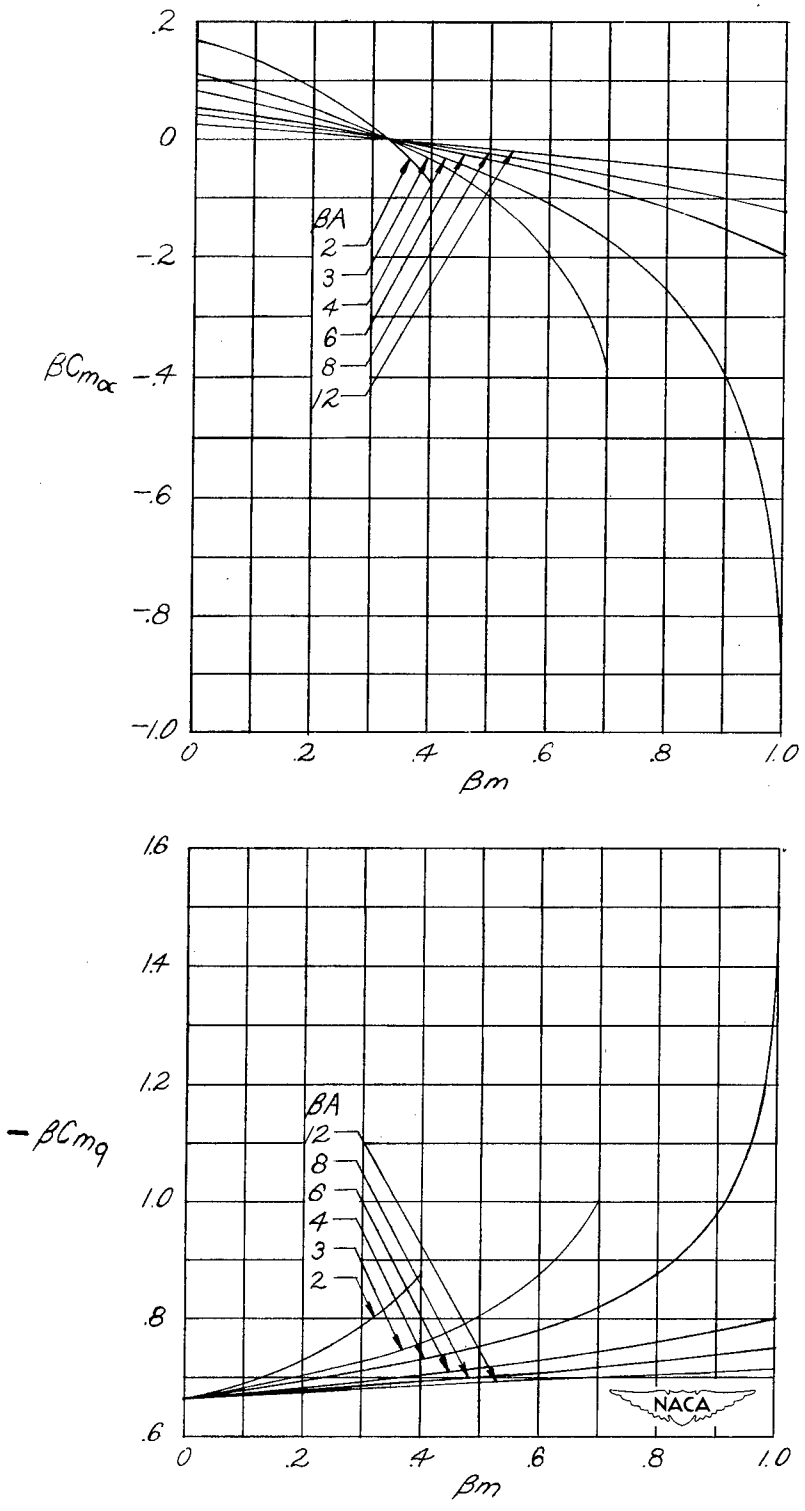

Figure 7.- Variation of βC_{m_α} and $-\beta C_{m_q}$ with βm for various values of βA for trapezoidal wings with raked-out tips.

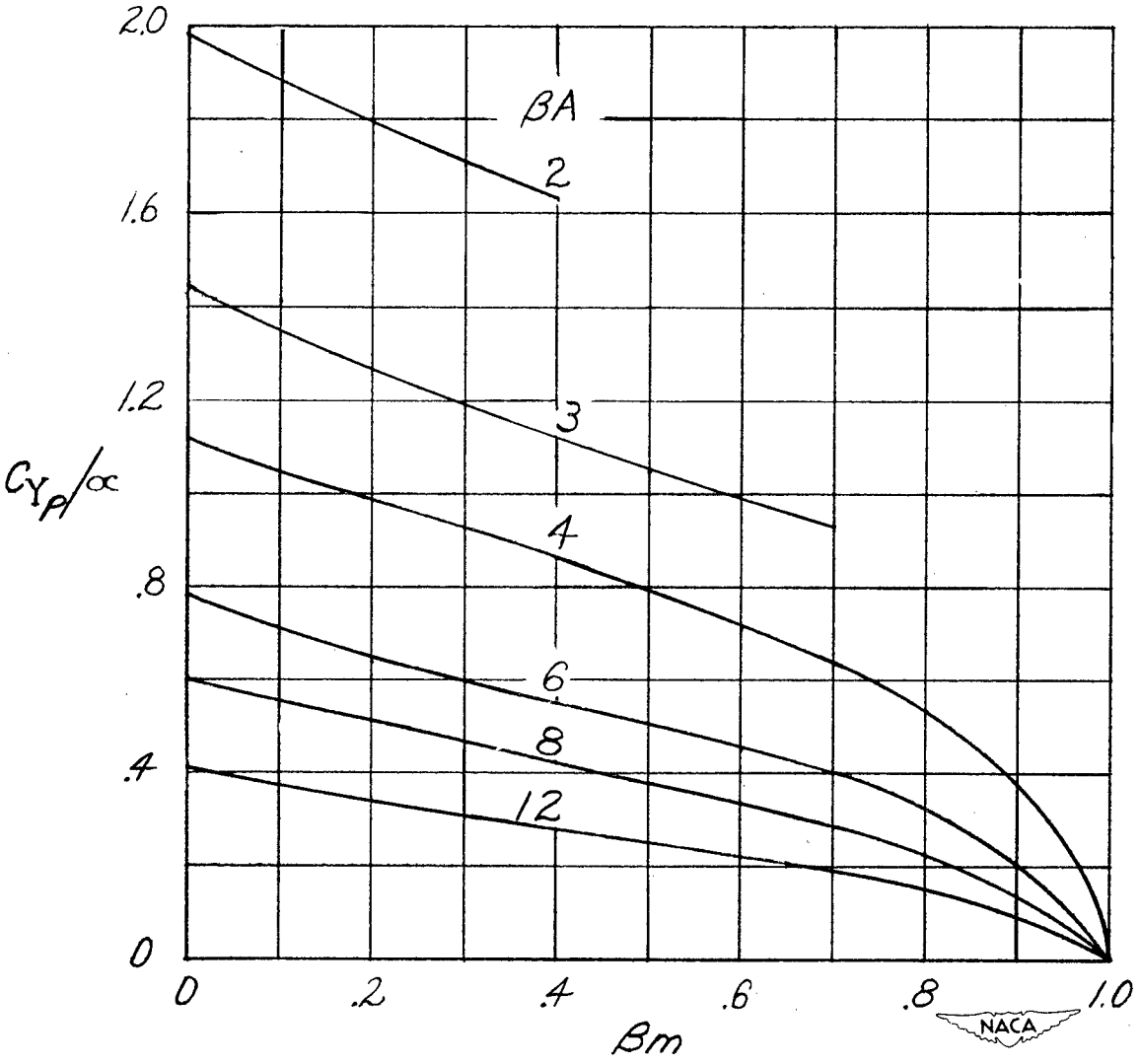

Figure 8.- Variation of C_{Y_p}/α with βm for various values of βA for trapezoidal wings with raked-out tips.

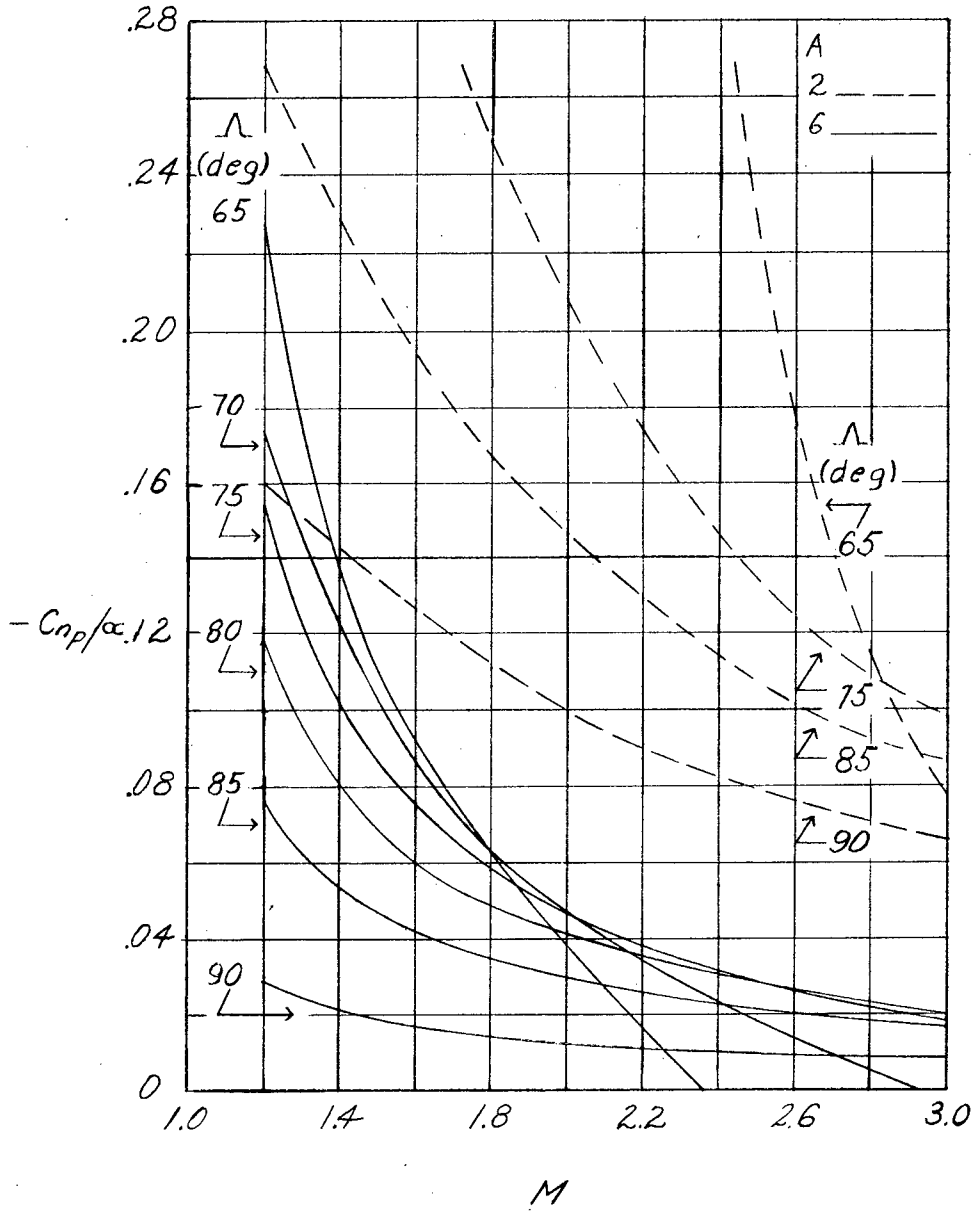

Figure 9.- Variation of $-C_{n_p}/\alpha$ with Mach number for various values of sweep angle for trapezoidal wings with raked-out tips.

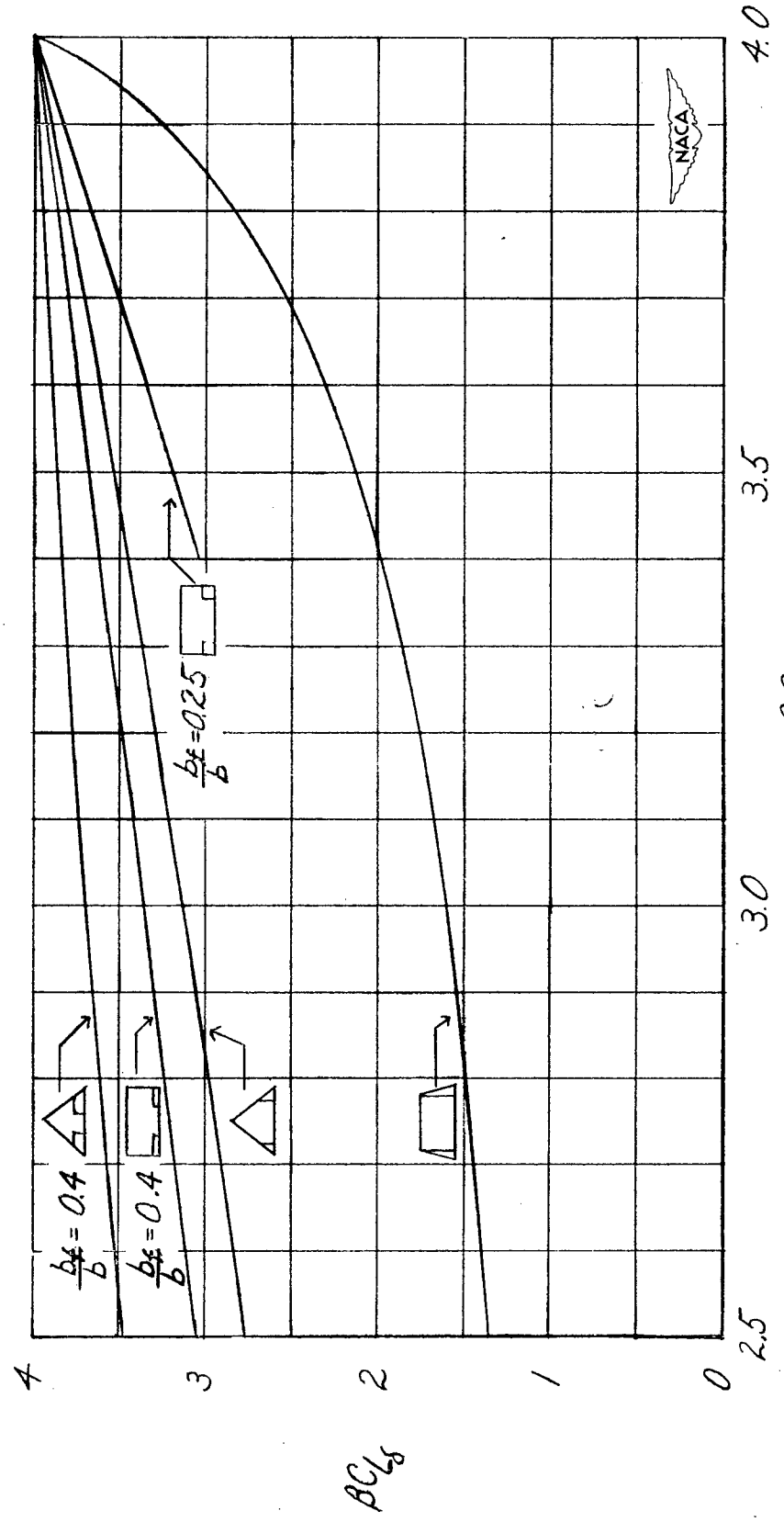

Figure 10.- Variation of βC_{L_δ} with βC_{L_α} for several wing-flap combinations. $\frac{S_f}{S}$ = 0.1.

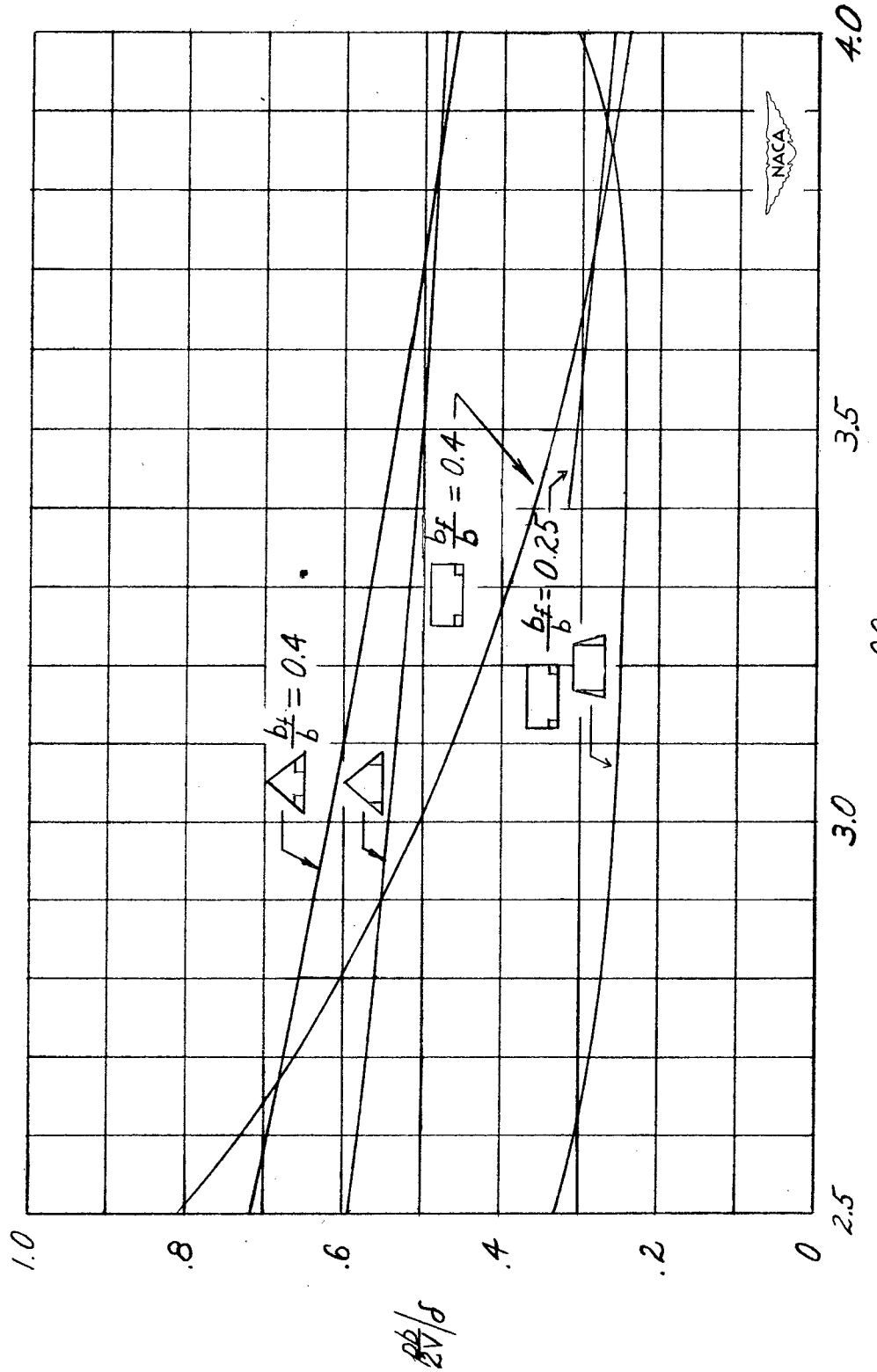

Figure 11.- Variation of $\frac{pb}{2V}/\delta$ with βC_{L_α} for several wing-flap combinations. $\frac{S_f}{S} = 0.1$.